# Catalytic growth in a shared enzyme pool ensures robust control of centrosome size

**Deb Sankar Banerjee**[1] **and Shiladitya Banerjee**[1,✉]

[1]Department of Physics, Carnegie Mellon University, Pittsburgh, PA 15213, USA

**Accurate regulation of centrosome size is essential for ensuring error-free cell division, and dysregulation of centrosome size has been linked to various pathologies, including developmental defects and cancer. While previous studies have mostly focused on investigating the growth dynamics of individual centrosomes, how a pair of centrosomes achieves equal size prior to cell division remains an open question. Here, we challenge the existing theory that centrosome growth is autocatalytic, as this model fails to explain the attainment of equal centrosome sizes. By incorporating recent experimental findings on the molecular mechanisms governing centrosome assembly, we propose a new mechanistic theory for centrosome growth involving catalytic assembly within a shared pool of enzymes. Our model successfully achieves robust size equality between maturing centrosome pairs, mirroring cooperative growth dynamics observed in experiments. To validate our theoretical predictions, we compare them with available experimental data and demonstrate the broad applicability of the catalytic growth model across different organisms, which exhibit distinct growth dynamics and size scaling characteristics.**

**organelle size control | organelle size scaling | centrosome assembly | limiting pool model | mathematical modeling**

Correspondence: *shiladtb@andrew.cmu.edu*

## Introduction

Centrosomes are membraneless organelles that act as microtubule organizing centers during mitotic spindle formation (1). Prior to cell division, centrosomes grow many folds in size by accumulating various types of proteins including microtubule nucleators, in a process known as centrosome maturation (2). Tight control of centrosome size is functionally important for the cell as aberrations in centrosome growth and size can lead to errors in chromosome segregation (3). This may result in aneuploidy, which is associated with a range of problems, including birth defects, developmental abnormalities, and cancer (4–6). Previous work has suggested that centrosomes grow cooperatively and regulate their size through a coordinated regulation of assembly and disassembly of the pericentriolic matter, mediated by a complex network of signaling pathways and regulatory proteins (7–10). Despite the significant progress on uncovering the molecular components regulating centrosome assembly (10), a quantitative model connecting the molecular mechanisms of growth to centrosome size regulation is lacking.

Centrosomes are composed of a porous scaffold-like structure (11, 12) known as the pericentriolic matter (PCM), organized around a pair of centrioles at the core (Fig. 1A). An individual cell starts with a single centrosome in the G1 phase, undergoes centriole duplication in the S phase, followed by the formation of two centrosomes in the G2/M phase (Fig. 1A). During centrosome maturation, the two spatially separated centrosomes grow to equal sizes by adding material to their PCMs from a finite pool of components (7, 13–16). Achieving equal size presents a challenge for the centrosome pair since small initial differences in the size could be amplified during the process of maturation, as the larger centrosome would incorporate more material on their surface, thereby outcompeting the smaller centrosome (17).

Previous models have described centrosome assembly as an autocatalytic process, assembled from a single limiting component that undergoes active phase segregation mediated by the chemical activity of the centriole (8). While this model quantitatively captures experimentally observed sigmoidal growth dynamics and the scaling of centrosome size with cell size, autocatalytic growth of centrosome pairs can induce significant size fluctuations. In recent work, we have shown that autocatalytic growth of multiple organelles in a shared pool of subunits results in organelle size inequality (18). This result is particularly relevant for understanding centrosome growth, as centrosome pairs grow from a shared pool of components during centrosome maturation (13). Furthermore, noise in the intracellular environment can induce centrosome size fluctuations, and the two centrosomes contain different centrioles (old mother centriole and new mother centriole, see Fig. 1A). These factors may introduce differences in centrosome size at the beginning of the maturation process. A robust size regulation mechanism is thus required to grow the two centrosomes to the same size, despite the presence of noise in growth and initial size differences.

Here we present a quantitative theory for size regulation of a centrosome pair via catalytic assembly from a shared pool of enzymes and molecular components. We first establish that autocatalytic growth of centrosomes in a shared subunit pool results in amplification of initial size differences, leading to significant size inequality after maturation. We then systematically investigate different models of centrosome size control based on known molecular design principles for centrosome assembly (10). In particular, a model for centriole-localized assembly and spatially distributed disassembly (18) ensures robust equality of centrosome size, while failing to capture sigmoidal growth curve as observed experimentally (13). Based on recent experiments uncovering the molecular components of centrosome assembly, we propose a new model of catalytic growth of centrosomes in a shared pool of enzymes. We show that this model ensures robust size control of centrosomes while capturing several key features

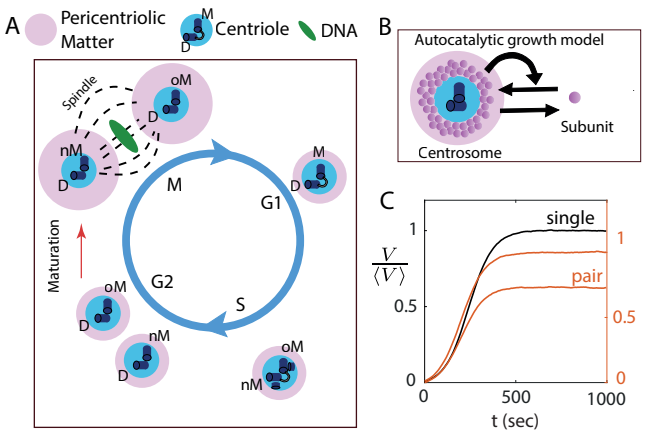


**Fig. 1. Autocatalytic feedback in centrosome growth drives centrosome size inequality.** (A) Schematic showing the dynamics of centrosomes during the cell cycle. In the G1 phase there is a single centrosome with mother (M) and daughter (D) centrioles at the core, surrounded by the pericentriolic matter (PCM). The two new centriole pairs with old mother (oM) and new mother (nM) separate into two centrosomes in the G2/M phase after centriole duplication. The spatially separated centrosomes then grow via a process called *centrosome maturation* (red arrow), prior cell division. (B) Schematic of the autocatalytic growth model for centrosomes, where the assembly rate increases with increasing centrosome size. (C) Autocatalytic growth of centrosomes captures the sigmoidal size dynamics for single and a pair of centrosomes, but unable to ensure size equality of a centrosome pair. See Table 1 for a list of parameter values.

of centrosome growth observed experimentally, including the growth of two stable centrosomes of equal size after maturation (10), sigmoidal growth dynamics (8, 13), tunable scaling of centrosome size with cell size (13), and the ability to robustly create centrosomes of different size from differences in centriole activity (19, 20).

## Results

### Autocatalytic feedback in centrosome growth drives centrosome size inequality

Previous work has suggested that centrosomes are autocatalytic droplets formed via active liquid-liquid phase separation (8). Autocatalytic growth arises if centrosome assembly rate increases with centrosome size, creating a size-dependent positive feedback (Fig. 1B). To investigate if autocatalytic growth can ensure size equality of centrosomes, we considered a model of centrosome growth via stochastic assembly and disassembly of its subunits. Though there are multiple essential components involved in PCM assembly (7, 21, 22), we first examined a one-component centrosome model to illustrate the role of autocatalytic growth on size control. The deterministic description for the growth of a pair of centrosomes can be written as

$$\frac{\mathrm{d}n_i}{\mathrm{d}t} = (k_0^+ + k_1^+ n_i(t))\rho(t) - k^- n_i(t)\,, \qquad \textbf{(1)}$$

where $n_i(t)$ is the amount of subunits in $i^{th}$ centrosome ($i = 1, 2$), $k_0^+$ and $k_1^+$ are the rate constants for non-cooperative and cooperative assembly, respectively, and $k^-$ is the disassembly rate constant. Eq. (1) can be derived from the phase segregation model for centrosome assembly studied by Zwicker *et al* (8) (see SI section I), with $k_0^+$ and $k_1^+$

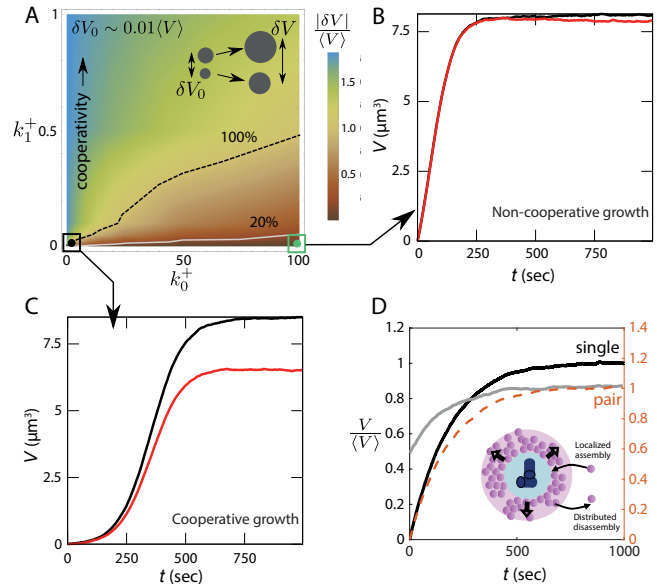


**Fig. 2. Lack of robust size control in autocatalytic growth.** (A) The relative difference in centrosome size, $|\delta V|/\langle V\rangle$, as a function of the growth rate constants $k_0^+$ and $k_1^+$, with an initial size difference of $0.1\ \mu\mathrm{m}^3$. The light gray and dashed black lines represent the lines $|\delta V|/\langle V\rangle = 0.2$ and $|\delta V|/\langle V\rangle = 1.0$. (B,C) Size dynamics of a pair centrosomes for (B) weakly cooperative ($k_0^+ = 100$, $k_1^+ = 0.001$) and (C) strongly cooperative ($k_0^+ = 0.1$, $k_1^+ = 0.001$) growth regimes. (D) Dynamics of centrosome size for a single centrosome and a pair of centrosomes simulated using the non-cooperative growth model. Inset: Schematic of centrosome growth via centriole-localized assembly and disassembly distributed throughout the PCM. The $|\delta V|/\langle V\rangle$ values in (A) represent average over $1000$ ensembles. The values of $k_0^+$ and $k_1^+$ are in the units of $\times 600\,\mu\mathrm{M}^{-1}\,s^{-1}$. See Table 1 for a list of parameter values.

representing centriole activity and the strength of autocatalytic interaction, respectively. In Eq. (1), $\rho(t)$ is the cytoplasmic concentration of centrosomal subunits, given by $\rho(t) = (N - n_1(t) - n_2(t))/V_c$ where $V_c$ is cell volume and $N$ is the total amount of subunits in the cell. Centrosome volume is given by $V_i(t) = n_i(t)\delta v$, where $\delta v$ is the effective volume occupied by a single subunit. As shown before (8), this model can capture the essential quantitative features of the growth of a single centrosome (Fig. 1C), including sigmoidal growth curve, temporal control of size and scaling of centrosome size with cell size. However, this model is unable to ensure size equality of two identical centrosomes growing from a shared subunit pool. Stochastic simulation shows significant difference in steady-state size even with a small initial size difference (Fig. 1C).

It is instructive to first compare two opposite limits of the model, $k_0^+ = 0$ (purely autocatalytic growth) and $k_1^+ = 0$ (non-cooperative growth). For $k_0^+ = 0$, Eq. (1) can be interpreted as assembly and disassembly occurring throughout the PCM volume, with the assembly rate scaling with centrosome size. As a result, the centrosome with a larger initial size would end up growing to a larger steady-state size. Stochastic simulations of this model show that the ensemble-averaged absolute difference in centrosome size ($|\delta V| = |V_1 - V_2|$) increases with the initial centrosome size difference ($\delta V_0$), indicating lack of robustness in size regulation (see SI section II and Fig. S1). On the other hand, the limit $k_1^+ = 0$ corresponds to a model where the assembly rate

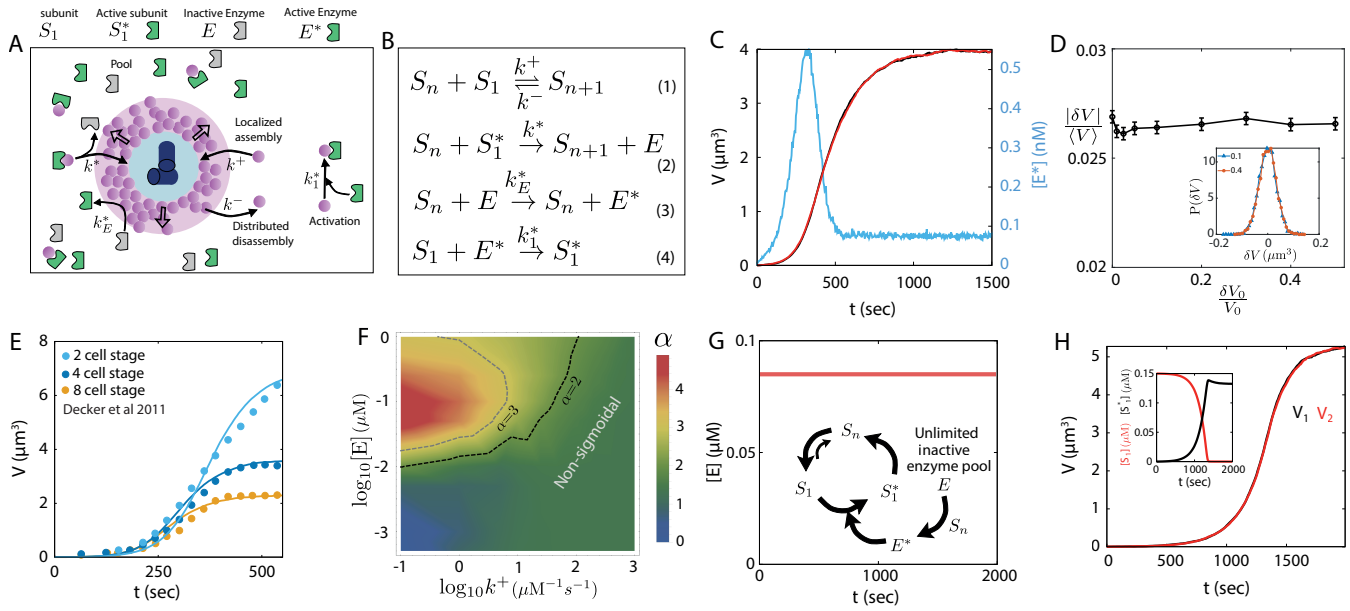


**Fig. 3. Catalytic growth in a shared enzyme pool leads to robust size control of a centrosome pair.** (A) Schematic of centrosome growth via catalytic activity of an enzyme that is activated by PCM proteins at a rate proportional to PCM size. (B) Reactions describing centrosome growth via catalytic activity of enzyme $E$. The centrosome ($S_n$) can activate the enzyme in a state $E^*$, which in turn creates an activated subunit ($S_1^*$) that binds the PCM. (C) Size dynamics of a centrosome pair (blue, red curves) growing via catalytic assembly and the dynamics of the activated enzyme ($[E^*]$) in time (blue curve). (D) The ensemble average of relative absolute size difference $|\delta V|/\langle V \rangle$ is insensitive to change in relative initial size difference $\delta V_0/V_0$. Inset: Probability distribution of $\delta V$ for two different values of initial size difference ($\delta V_0/V_0 = 0.1$ and $\delta V_0/V_0 = 0.4$). (E) Centrosome growth curves obtained from the catalytic growth model (lines) fitted to experimental growth curves (points) measured at different stages of *C. elegans* development. (F) Degree of sigmoidal growth, measured by Hill coefficient $\alpha$, as a function of the growth rate constant $k^+$ and the total enzyme concentration $[E]$. (G) Model of shared catalysis considering a constant concentration of inactive enzyme ($E$) throughout the growth period. Inset: Schematic of the reactions showing the steady state cycle between $S_1$, $S_1^*$ and $S_n$. (H) Centrosome pair growth in the presence of unlimited inactive enzyme pool exhibits size equality as well as cooperative growth dynamics. Inset: Dynamics of $S_1$ and $S_1^*$ concentrations. See Table 1 for a list of parameter values.

is constant, and material turnover is distributed throughout the PCM volume. This model guarantees size equality of a centrosome pair competing for a limiting subunit pool (see SI section II and Fig. S2), even in the presence of large initial size differences (Fig. 2D), with the steady-state size given by $V = k^+ N \delta v/(k^- + 2k^+)$. While this growth model captures centrosome size equality and centrosome size scaling with cell size (18), the resulting growth curve is non-sigmoidal, in contrast to experimental data in *C. elegans* (8, 13).

To quantify the robustness of size control, we measured the relative difference in steady-state centrosome size, $|\delta V|/\langle V \rangle$, starting with an initial size difference $\delta V_0 \sim 0.01\langle V \rangle$, where $|..|$ denotes the absolute value and $\langle V \rangle$ is the ensemble average of centrosome size at steady-state. The resulting size inequality is controlled by the rate constants $k_0^+$ and $k_1^+$. Our analysis shows that there is a relatively small region of the parameter space where the strength of the autocatalytic feedback is low enough (i.e., $k_0^+ \gg k_1^+$) to ensure small difference in centrosome size (Fig. 2A). However, in this range of parameter values, the growth is essentially non-cooperative and the growth curve is not sigmoidal (Fig. 2B). Larger size inequality is associated with higher values of $k_1^+$, when the growth dynamics is sigmoidal in nature (Fig. 2C). Furthermore, size inequality in centrosome growth occurs in a biologically relevant time-scale ($\sim 500 - 1000$ s (8, 13)). The loss of size regulation as well as the lack of sigmoidal growth of a centrosome pair is not sensitive to the initial size difference, as even with small relative size difference the absolute difference in size can still be large (Fig. S3).

**Catalytic growth in a shared enzyme pool ensures centrosome size equality while maintaining cooperative growth**

Centrosome growth during maturation occurs through the expansion of a scaffold-like structure and subsequent recruitment of PCM proteins on the scaffold. While multiple proteins are involved in the scaffold assembly, Spd-2 and centrosomin (Cnn) are two essential scaffold forming proteins, in the absence of which centrosome growth is almost entirely diminished (7). The kinase Polo interacts with both Spd-2 and Cnn to promote the assembly of a stable scaffold. In particular, Spd-2 recruits Cnn with the help of Polo and Cnn in turn strengthens the Spd-2 scaffold without directly recruiting additional Spd-2 proteins. Without the Polo kinase, the Cnn scaffold fails to grow (9). These findings suggest a model for catalytic assembly of centrosomes based on positive feedback between scaffold-forming proteins and an enzyme. To test if such a model can promote cooperative growth while ensuring size equality of a centrosome pair, we first developed a single-component model for PCM growth catalyzed by an enzyme (Fig. 3A).

In this single-component model, the PCM is composed of a single type of subunit that can either take an inactive form ($S_1$), or an enzyme-dependent active form ($S_1^*$), with $S_n$ representing a centrosome with $n$ subunits. The single coarse-grained subunit ($S_1$) represents a composite of the scaffold-forming proteins (e.g., Spd-2 and Cnn in *Drosophila*), and the enzyme ($E$) represents the kinase (e.g., Polo in *Drosophila*). The inactive subunit can slowly bind and unbind from the

PCM, while the enzyme-activated form can assemble faster (reactions 1 and 2 in Fig. 3B). The subunit activation is carried out by the active form of the enzyme ($E^*$). Enzyme activation occurs in the PCM, and is thus centrosome size-dependent (reactions 3 and 4 in Fig. 3B). A centrosome with a larger PCM thus produces active enzymes at a faster rate, and an increased amount of activated enzymes enhance centrosome growth. Thus, size-dependent enzyme activation generates a positive feedback in growth, which is shared between the centrosomes as the enzymes activated by each centrosome become part of the shared enzyme pool. This is in contrast to the autocatalytic growth model where the size-dependent positive feedback was exclusive to each centrosome.

Using the above described dynamics (Fig. 3B), we performed stochastic simulations of a pair of centrosomes growing from a shared pool of enzymes and subunits. The resulting growth dynamics are sigmoidal, and lead to equally sized centrosomes (Fig. 3C). Interestingly, the dynamics of the activated enzyme show an *activation pulse* at the onset of growth (Fig. 3C), similar to the experimentally observed Polo pulse that initiates centrosome assembly in *Drosophila* (23). This pulse in the cytoplasmic concentration of active enzymes arises from the dynamics of enzyme activation by the PCM scaffold and its subsequent consumption by PCM subunits. The amplitude and the lifetime of the pulse depend on the difference in the timescales of enzyme activation and consumption (Fig. S4). The experimentally observed Polo pulse is regulated by the abundance of the centriolar protein Ana1 (23), which controls the enzyme activation rate ($k_E^*$) in our model. Exploring the effect of this activation rate, we observe increased pulse period and decreased pulse amplitude with decreasing enzyme activation rate (Fig. S4). These results are markedly similar to the experimentally observed effect of reduced Ana1, which reduces the overall rate of Polo activation in the centrosome (23).

Importantly, this model ensures robustness in centrosome size equality, with a negligible difference in steady-state size ($\sim 2\%$ of mean size) that is independent of the initial size difference (Fig. 3D). The difference in steady-state size is a result of the fluctuations in the individual centrosome size dynamics, as evident from the distribution of the size difference (Fig. 3D-inset). We find that the centrosome growth dynamics predicted by this model match really well with the experimental growth curves in *C. elegans* (13) (Fig. 3E).

Though centrosome growth in *C. elegans* is found to be sigmoidal, it has been suggested that centrosomes in *Drosophila* grow in a non-sigmoidal fashion (8). Although we could not find any direct quantitative measurement of centrosome size dynamics in *Drosophila* or other organisms, analysis of PCM assembly dynamics using flourescence reporters show varying degrees of cooperativity during *Drosophila* development (23). We therefore sought to explore whether our catalytic growth model can also describe non-sigmoidal growth. To this end, we characterized the sigmoidal nature of the growth by fitting the dynamics of centrosome volume $V(t)$ to a Hill function of the form $At^\alpha/(B^\alpha + t^\alpha)$, where the coefficient $\alpha$ represents the strength of cooperativity. Our results show that the cooperative nature of growth depends on the interplay between the growth rate constant $k^+$ and the total enzyme concentration $[E]$, such that growth is sigmoidal ($\alpha \geq 2$) for larger $[E]$ and smaller $k^+$, and non-sigmoidal otherwise (Fig. 3F).

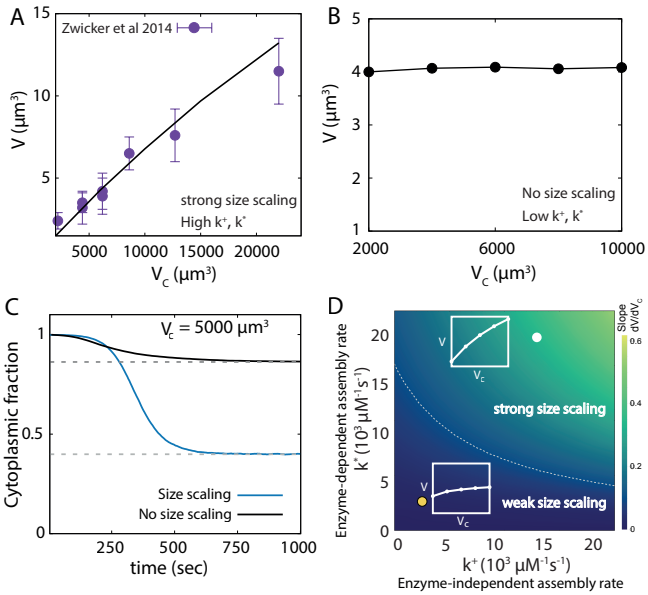


**Fig. 4. Centrosome size scaling with cell size.** (A) Scaling of centrosome size with cell size obtained from the catalytic growth model (line) fitted to experimental data (points) in *C. elegans* embryo (8). (B) Centrosome size does not scale with cell size when the assembly rates are much lower compared to disassembly rate (i.e., $k^*, k^+ \lesssim k^- V_c$). (C) Dynamics of the cytoplasmic fraction of subunits ($S_1$ and $S_1^*$ combined) reveal significantly higher pool depletion in the size scaling regimes. The two curves correspond to the growth curves shown in panels A (blue) and B (black). The dashed lines are theoretical results obtained from the deterministic model. (D) An analytically obtained phase diagram of centrosome size scaling as functions of enzyme-dependent and enzyme-independent assembly rate constants. The color indicates the strength of size scaling (measured by $dV/dV_c$). The dashed gray line indicates the contour $dV/dV_c = 0.1$. Here the slope values are shown in $\delta v$ units. Insets: Characteristic size scaling behaviours. See Table 1 for a list of parameter values.

While our model of shared catalysis considers a limiting pool of enzymes, a finite enzyme pool is not required for robust size control. To show this, we considered an unlimited pool inactive enzymes ($E$), such that the cytoplasmic concentration of $E$ does not change over time (Fig. 3G). The unlimited pool of inactive enzymes keeps producing activated enzymes via the centrosomes. The centrosome size reaches a steady-state when the subunit activation (via $E^*$) and subsequent growth is balanced by subunit disassembly from the centrosome (Fig. 3G-inset). The size equality and cooperativity of growth remain intact in the presence of constant $[E]$ (Fig. 3H). The prevalence of activated enzyme almost entirely depletes the inactive subunit pool and the centrosomes are in chemical equilibrium with the active subunit pool in the steady state (Fig. 3H-inset).

## Cytoplasmic pool depletion regulates centrosome size scaling with cell size

Since our model for centrosome growth is limited by a finite amount of subunits, it is capable of capturing centrosome size scaling with cell size (Fig. 4A), in excellent agreement with

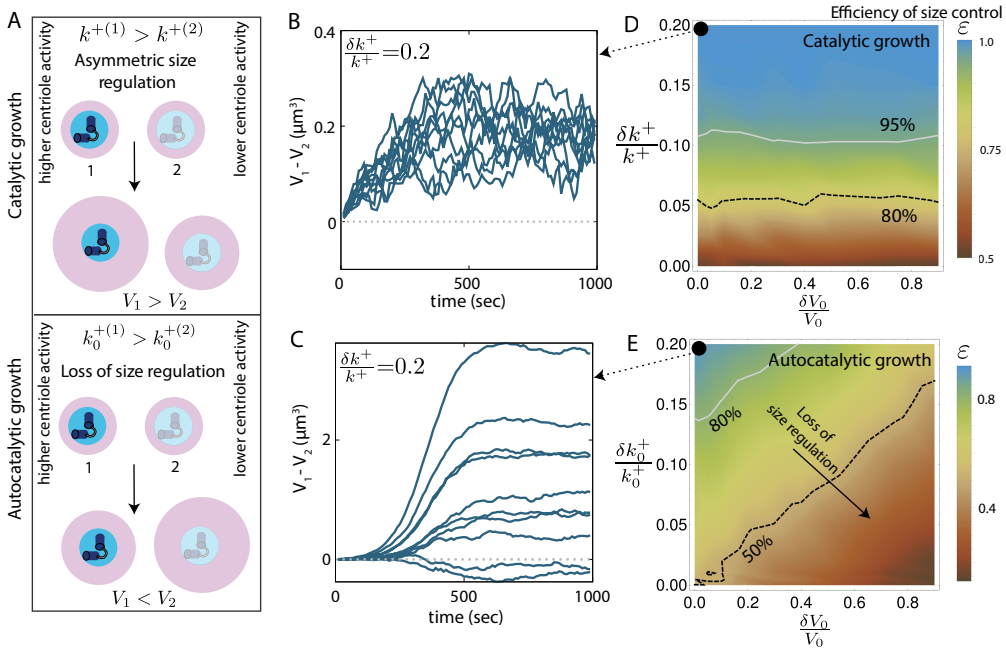


**Fig. 5. Control of centrosome size asymmetry via differential growth.** (A) Schematic illustrating asymmetric size regulation via differential growth in the (top) catalytic growth model and (bottom) autocatalytic growth model. (B,C) Ten representative trajectories showing the dynamics of centrosome size difference ($V_1 - V_2$) for (B) catalytic growth model ($\delta k^+/k^+ = 0.2$), and (C) autocatalytic growth model ($\delta k_0^+/k_0^+ = 0.2$). The two centrosomes are initially of the same size. (D) Efficiency growth-rate-dependent control of centrosome size asymmetry ($\varepsilon = N^+/N_{\text{tot}}$) as a function of (normalized) initial size difference ($\delta V_0/V_0$) and (normalized) growth rate difference ($\delta k^+/k^+$), in the catalytic growth model. (E) Efficiency of growth-rate-dependent control of centrosome size asymmetry as a function of (normalized) initial size difference ($\delta V_0/V_0$) and (normalized) growth rate difference ($\delta k_0^+/k_0^+$), in the autocatalytic growth model. See Table 1 for a list of model parameters.

experimental data (8, 13). However, the extent of organelle size scaling with cell size depends on the assembly rate and becomes negligible when the assembly rate is not significantly higher compared to the disassembly rate (Fig. 4B). In particular, centrosome size scaling is connected to the extent of subunit pool depletion, such that the steady-state cytoplasmic fraction of the subunits is low when centrosome size scales with the cell size and higher otherwise (Fig. 4C).

To understand how size scaling is regulated by growth parameters, we derived a simplified analytical form (see SI section III) for the steady-state centrosome size given by

$$V = \frac{(E^* k_1^* + k^+) k^* \rho_0 V_c \delta v}{k^*(k^+ + k^- V_c) + E^* k_1^*(k^* + k^- V_c)}, \qquad (2)$$

where $\delta v$ is the volume occupied by a centrosome subunit, $\rho_0$ is the total subunit density, and the enzymes are assumed to reach their steady-state abundance $E^*$ very fast. From the above expression, we can see that centrosome size $V$ will strongly scale with cell size $V_c$ when $k^+, k^* \gg k^- V_c$. This result is reflected in the phase diagram of size scaling (measured as the slope $\sim \mathrm{d}V/\mathrm{d}V_c$), which shows stronger size scaling with increasing assembly rates (Fig. 4D). The subunit pool depletion also increases with the assembly rates, reaching a state of almost complete depletion (i.e., $V \to \rho_0 V_c \delta v$) as we approach the regime of strong size scaling (see Fig. S5). It is important to note here that size scaling with cell size reported here is different from the linear size scaling predicted by the canonical limiting pool model (13, 24). Robust size control for multiple centrosomes requires size-dependent negative feedback and with this feedback, the size scaling with cell size becomes a feature achieved in a range of cell volumes by tuning growth rates. Interestingly, strong size scaling has been observed in *C. elegans* embryos (13), which are smaller in size ($\sim 10^4\,\mu\mathrm{m}^3$) than Drosophila embryos ($\sim 10^6\,\mu\mathrm{m}^3$) that do not exhibit size scaling with centrosome number (inferred from intensity data in (23)). This feature can be explained by our model in the regime of weaker size scaling, which is expected for larger system sizes (see SI section III & Fig. S5). Thus, the parameters of our model can be tuned to capture both sigmoidal and non-sigmoidal growth and strong or weak size scaling, without changing the nature of the molecular interactions that are largely conserved across organisms (17).

## Control of centrosome size asymmetry through differential growth

An essential aspect of centrosome size regulation is the modulation of centrosome size by centriole activity. In particular, it has been shown that the centrosome associated with a more active centriole will grow larger, resulting in centrosomes of unequal size (19, 20). Control of centriole activity-driven centrosome size asymmetry is important as this size asymmetry may play a crucial role in stem cell division as observed in *Drosophila* neuroblasts (19). We test the effectiveness of size regulation by studying the growth of a centrosome pair with different centriole activities, controlled by the values of the growth rate constants $k_0^+$ and $k^+$ for the autocatalytic (Eq. 1) and the catalytic (Fig. 3B) growth models, respectively (Fig. 5A). For both the models, we bias the initial size of the centrosomes by assigning a smaller initial size ($V_0 - \delta V_0$) to the centrosome with a higher centriole activity (i.e., $k_0^{+(1)} = k_0^+ + \delta k_0^+$ or $k^{+(1)} = k^+ + \delta k^+$). We then

simulate the growth of $N_{\text{tot}}$ centrosome pairs and quantify the efficiency ($\varepsilon$) of size control as the ratio of the number of cases ($N^+$) where the centrosome with higher growth rate ($k_0^+ + \delta k_0^+$ or $k^+ + \delta k^+$) becomes larger, to the total number of simulated pairs, $\varepsilon = N^+/N_{\text{tot}}$.

In the absence of any initial size difference ($\delta V_0 = 0$), the catalytic growth model shows better control of differential growth-induced size asymmetry (Fig. 5B), while the autocatalytic growth model shows wide variations in centrosome size difference (Fig. 5C). We find that the catalytic growth model ensures that the centrosome with a larger $k^+$ (higher centriole activity) end up being larger, irrespective of the initial size difference (Fig. 5D). This illustrates robust control of centrosome size asymmetry by controlling differences in centriole activity. By contrast, in the autocatalytic growth model, the efficiency of size control monotonically decreases with increasing initial size difference, reflecting the lack of robustness in size control (Fig. 5E).

**Multi-component centrosome model reveals the utility of shared catalysis on centrosome size control**

One major postulate of the one-component PCM model was that the enzyme pool was shared between the two centrosomes rather than being localized to each. Here we support this assumption using a multi-component centrosome model that allows us to model the specific interactions between the enzyme and the centrosome components. Based on recent studies (9, 10), we model the centrosomes with two essential scaffold-forming proteins, $a$ and $b$, whose assembly into the PCM scaffold is regulated by the kinase $E$. The total size of the PCM scaffold, $S$, and the centrosome volume $V$ are given by $S = S(a) + S(b)$ and $V = V_a + V_b$, where $S(a)$ ($S(b)$) and $V_a$ ($V_b$) denote the contribution to the scaffold size (in number of subunits) and the centrosome volume by the component $a$ ($b$). The molecular identities of these key components are listed in Table 2 for different organisms. In particular, for *Drosophila*, $a$ and $b$ can be identified as the scaffold forming proteins Spd-2 and Cnn, while $E$ represents the kinase Polo. It has been observed that Spd-2 and Cnn cooperatively form the PCM scaffold to recruit almost all other proteins involved in centrosome maturation (7). To effectively coordinate cooperative growth of the scaffold, Spd-2 proteins recruit the kinase Polo, which in turn phosphorylates Cnn at the centrosome (9). In the absence of Polo, Cnn proteins can bind to the scaffold but fall off rapidly, leading to diminished centrosome maturation (9, 25).

We incorporated these experimental observations in our multi-component model as described in Fig. 6A. We then test two different models for enzyme spatial distribution: (i) enzyme $E$ (Polo) is activated at each centrosome by the scaffold component $a$ (Spd-2), which then assembles the second component $b$ (Cnn) into the scaffold of that particular centrosome (for details see SI Section IVA), and (ii) enzyme $E$ activated by the scaffold component $a$ is released in the cytoplasmic pool, promoting assembly of the $b$-scaffold at both centrosomes (for details see SI Section IVB). In the first case, localized enzyme interaction exclusively enhances the growth

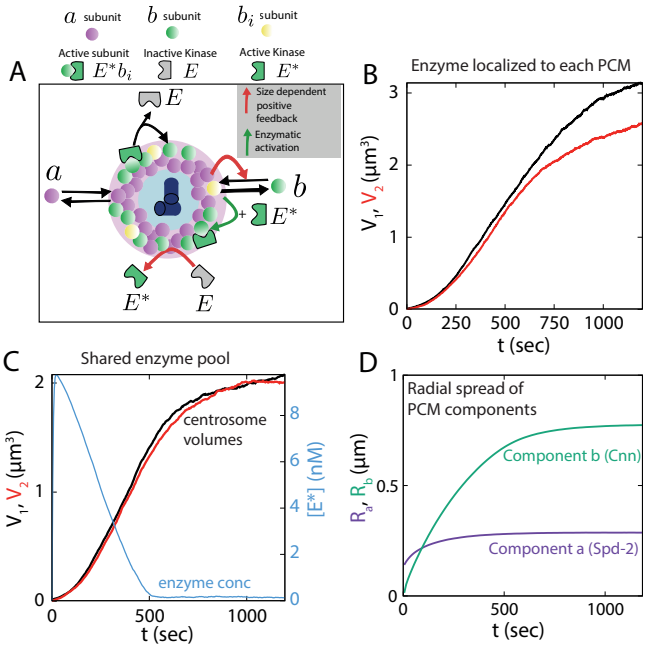


**Fig. 6. Multi-component model for centrosome growth.** (A) Schematic of centrosome growth model driven by two scaffold components $a$ and $b$, and enzyme E. $a$ can bind the existing PCM independent of $b$ or the enzyme $E$. The enzyme is activated by $a$ in the scaffold, then released in the cytoplasm as $E^*$. The other scaffold former $b$ binds to PCM in $a$-dependent manner in an intermediate form $b_i$ which can undergo rapid disassembly. The intermediate form $b_i$ can get incorporated in the $b$-scaffold by the active enzyme $E^*$ via forming an activated subunit form $E^*b_i$. The red arrows indicate the size dependent positive feedback and the green arrow indicates the catalytic activity of the enzyme. (B) Centrosome size ($V_1, V_2$) dynamics for growth with localized enzyme. (C) Centrosome size ($V_1, V_2$) dynamics for growth with shared enzyme pool (black and red curve) and the pulse-like dynamics of activated enzyme concentration ($[E^*]$, blue curve). (D) Radial spread of the two scaffold former components $a$ and $b$ corresponding to the centrosome growth shown in panel-C. See Table 1 for a list of parameter values.

of the individual centrosomes, creating an autocatalytic feedback that leads to size inequality of centrosomes (Fig. 6B). Similar to model Eq. (1), the steady-state size difference between the two centrosomes increases with the increasing initial size difference, resulting in a failure of robust size control (Fig. S6).

We then considered the second case where the enzyme-mediated catalysis is shared between the growing centrosome pair. Experimental observations suggest a dynamic enzyme population around the centrosomes (26, 27), with a turnover timescale much smaller than the scaffold forming proteins (7, 28). These findings point towards the possibility that the enzyme is transiently localized in the centrosome during activation and the active enzyme is then released in the cytoplasmic pool that can enhance the growth of both the centrosomes (Fig. 6A). We incorporate this shared catalysis mechanism in the second model where $a$ activates the enzyme to $E^*$ which then gets released in the cytoplasm, facilitating $b$-scaffold expansion in both the centrosomes (see SI Section IVB for details). This growth mechanism is able to robustly control centrosome size equality (Fig. S7), giving rise to the characteristic sigmoidal growth dynamics (Fig. 6C), where the first scaffold former $a$ is smaller in amount than the second, enzyme-aided component $b$. This difference in the abundances of $a$ and $b$ proteins, when trans-

lated into their respective radial spread from the centrosome center ($R \propto V^{1/3}$), bears close resemblance with the relative spread in Spd-2 and Cnn observed in the experiments, where the Cnn spread is twice as large as Spd-2 (7, 9) (Fig. 6D). The active enzyme dynamics also resembles the observed pulse in Polo dynamics at the beginning of centrosome maturation (23) (Fig. 6C). Overall, the two-component model provides crucial insights into the role of shared catalytic growth on centrosome size control and lays the theoretical foundation for further investigations into the molecular processes that govern centrosome assembly.

## Discussion

In this article, we examined quantitative models for centrosome growth via assembly and disassembly of its constituent building blocks to understand how centrosome size is regulated during maturation. Previous studies (7–10, 25, 29) have suggested that centrosome assembly is cooperative, and an autocatalytic growth model (8) quantitatively explains the cooperative growth dynamics of individual centrosomes. However, as we showed here, an autocatalytic growth model does not guarantee the size equality of two centrosomes growing from a shared subunit pool. The resultant size inequality increases with the initial size difference between the centrosomes, indicating a lack of robustness in size control.

Following recent experiments on the molecular mechanisms of centrosome assembly, we constructed an enzyme-mediated catalytic growth model that not only describes cooperative growth behavior but also ensures robustness in size equality of the two maturing centrosomes. The enzyme Polo-like kinase (PLK1) that coordinates centrosome growth (9, 25, 29, 30), has a much faster turnover rate ($\sim 10$ seconds) than the centrosome scaffold forming proteins Spd-2 and Cnn (7, 28). This leads us to hypothesize that the kinase which is activated at the centrosome may get released in the cytoplasm, becoming part of a shared pool of enzymes that catalyzes the growth of both centrosomes without any bias. We demonstrated that this mechanism of shared catalysis can robustly regulate centrosome size despite intracellular noise and variability in growth dynamics. It maybe likely that all components of centrosome growth may not be limited in a cell. To this end, we show that a limiting pool of enzyme is not strictly required for robust size control of centrosomes.

We subsequently extended our single-component model of catalytic growth to a multi-component model involving PCM scaffold-forming proteins (Spd-2 and Cnn in Drosophila) and the enzyme Polo kinase. Using this model, we explicitly tested the hypothesis that a shared enzyme pool is required to achieve robust size control and showed that a localized catalysis model leads to size differences in mitotic centrosomes. Consistent with recent experimental observations that PLK1 concentration can regulate centrosome size (30), we find that centrosome size increases with increasing enzyme concentration and that centrosome growth is inhibited in the absence of the enzyme (Fig. S7). Since the activity of the Polo kinase is cell-cycle dependent (31, 32), we further explored the dynamics of centrosome growth with a time-dependent dynamics of the enzyme. We found that centrosome growth can be triggered by switching on the enzyme dynamics and centrosome size was reduced when the enzyme was switched off (Fig. S7). Importantly, it supported the experimental observation that a continuous Polo activity is required to maintain the PCM scaffold (26, 33).

Many key features of centrosome growth such as the sigmoidal growth curve and size scaling behavior can be modulated in our model by changing the growth rate constants and enzyme concentration, while conserving the underlying molecular mechanisms for assembly. This opens up the possibility that the catalytic growth model may be broadly relevant to other organisms where homologous proteins (Table 2) play similar functional roles in regulating centrosome growth (10). Aside from capturing the existing data on the dynamics of centrosome growth, our catalytic growth model makes several other predictions that can be tested in future experiments. These include, increasing the cooperativity of growth dynamics by increasing enzyme concentration or reducing binding rate of subunits to PCM, inducing a transition from strong size scaling to weak size scaling by lowering the assembly rate or by reducing pool depletion. Following the dynamics two centrosomes of unequal size during the initial phase of the maturation process can be a direct test of robustness in centrosome size control. The catalytic growth model also predicts that the final size difference of the centrosomes will be independent of the initial size difference, that can be tested in experiments. Additionally, the prediction of centrosome size being strongly correlated with enzyme concentration can be experimentally tested by changing the cytoplasmic concentration of Polo kinase.

## References


1. Roy R Gould and Gary G Borisy. The pericentriolar material in chinese hamster ovary cells nucleates microtubule formation. *The Journal of cell biology*, 73(3):601–615, 1977.
2. Robert E Palazzo, Jacalyn M Vogel, Bradley J Schnackenberg, Dawn R Hull, and Xingyong Wu. Centrosome maturation. *Current topics in developmental biology*, 49:449–470, 1999.
3. A Krämer, K Neben, and AD Ho. Centrosome replication, genomic instability and cancer. *Leukemia*, 16(5):767–775, 2002.
4. Antonino B D'Assoro, Wilma L Lingle, and Jeffrey L Salisbury. Centrosome amplification and the development of cancer. *Oncogene*, 21(40):6146–6153, 2002.
5. Renata Basto, Kathrin Brunk, Tatiana Vinadogrova, Nina Peel, Anna Franz, Alexey Khodjakov, and Jordan W Raff. Centrosome amplification can initiate tumorigenesis in flies. *Cell*, 133(6):1032–1042, 2008.
6. Michelle S Levine, Bjorn Bakker, Bram Boeckx, Julia Moyett, James Lu, Benjamin Vitre, Diana C Spierings, Peter M Lansdorp, Don W Cleveland, Diether Lambrechts, et al. Centrosome amplification is sufficient to promote spontaneous tumorigenesis in mammals. *Developmental cell*, 40(3):313–322, 2017.
7. P T Conduit, Jennifer H Richens, Alan Wainman, James Holder, Catarina C Vicente, Metta B Pratt, Carly I Dix, Zsofia A Novak, Ian M Dobbie, Lothar Schermelleh, and Jordan W Raff. A molecular mechanism of mitotic centrosome assembly in drosophila. *eLife*, 3(e03399), 2014.
8. D Zwicker, M Decker, S Jaensch, A A Hyman, and F Jülicher. Centrosomes are autocatalytic droplets of pericentriolar material organized by centrioles. *Proc Natl Acad Sci*, 111:E2636–2645, 2014.
9. Ines Alvarez-Rodrigo, Thomas L Steinacker, Saroj Saurya, Paul T Conduit, Janina Baumbach, Zsofia A Novak, Mustafa G Aydogan, Alan Wainman, and Jordan W Raff. Evidence that a positive feedback loop drives centrosome maturation in fly embryos. *Elife*, 8, 2019.
10. Paul T Conduit, Alan Wainman, and Jordan W Raff. Centrosome function and assembly in animal cells. *Nature reviews Molecular cell biology*, 16(10):611–624, 2015.
11. Bradley J Schnackenberg, Alexey Khodjakov, Conly L Rieder, and Robert E Palazzo. The disassembly and reassembly of functional centrosomes in vitro. *Proceedings of the National Academy of Sciences*, 95(16):9295–9300, 1998.
12. Zhe Feng, Anna Caballe, Alan Wainman, Steven Johnson, Andreas F.M. Haensele, Matthew A. Cottee, Paul T. Conduit, Susan M. Lea, and Jordan W. Raff. Structural basis for mitotic centrosome assembly in flies. *Cell*, 169:1078–1089, 2017.
13. Markus Decker, Steffen Jaensch, Andrei Pozniakovsky, Andrea Zinke, Kevin F. O'Connell, Wolfgang Zachariae, Eugene Myers, and Anthony A. Hyman. Limiting amounts of centro-

some material set centrosome size in c. elegans embryos. *Current Biology*, 21(6):1259–1267, 2011.
14. J. B. Woodruff, O. Wueseke, and A. A. Hyman. Pericentriolar material structure and dynamics. *Philos. Trans. R. Soc. Lond.*, B 369(20130459), 2014.
15. C.A. Kemp, K.R. Kopish, P. Zipperlen, J. Ahringer, and K.F. O'Connell. Centrosome maturation and duplication in c. elegans require the coiled-coil protein spd-2. *Dev. Cell*, 6:511–523, 2004.
16. L. Pelletier, N. Ozlü, E. Hannak, C. Cowan, B. Habermann, M. Ruer, T. Müller-Reichert, and A.A. Hyman. The caenorhabditis elegans centrosomal protein spd-2 is required for both pericentriolar material recruitment and centriole duplication. *Curr. Biol.*, 14:863–873, 2004.
17. Jordan W Raff. Phase separation and the centrosome: a fait accompli? *Trends in Cell Biology*, 2019.
18. Deb Sankar Banerjee and Shiladitya Banerjee. Size regulation of multiple organelles competing for a limiting subunit pool. *PLOS Computational Biology*, 18(6):e1010253, 2022.
19. Paul T Conduit and Jordan W Raff. Cnn dynamics drive centrosome size asymmetry to ensure daughter centriole retention in drosophila neuroblasts. *Current Biology*, 20(24):2187–2192, 2010.
20. J Januschke, J Reina, S Llamazares, T Bertran, F Rossi, J Roig, and C Gonzalez. Centrobin controls mother–daughter centriole asymmetry in drosophila neuroblasts. *Nature cell biology*, 15(3):241–248, 2013.
21. Jeroen Dobbelaere, Filipe Josue, Saskia Suijkerbuijk, Buzz Baum, Nicolas Tapon, and Jordan Raff. A genome-wide rnai screen to dissect centriole duplication and centrosome maturation in drosophila. *PLoS biology*, 6(9):e224, 2008.
22. P T Conduit, K Brunk, J Dobbelaere, C I Dix, E P Lucas, and J W Raff. Centrioles regulate centrosome size by controlling the rate of cnn incorporation into the pcm. *Curr. Biol*, 20: 2178–2186, 2010.
23. Siu-Shing Wong, Zachary M Wilmott, Saroj Saurya, Ines Alvarez-Rodrigo, Felix Y Zhou, Kwai-Yin Chau, Alain Goriely, and Jordan W Raff. Centrioles generate a local pulse of polo/plk1 activity to initiate mitotic centrosome assembly. *The EMBO Journal*, 41(11): e110891, 2022.
24. Nathan W Goehring and Anthony A Hyman. Organelle growth control through limiting pools of cytoplasmic components. *Curr. Biol.*, 22(9):R330–R339, 2012.
25. Jeffrey B Woodruff, Oliver Wueseke, Valeria Viscardi, Julia Mahamid, Stacy D Ochoa, Jakob Bunkenborg, Per O Widlund, Andrei Pozniakovsky, Esther Zanin, Shirin Bahmanyar, et al. Regulated assembly of a supramolecular centrosome scaffold in vitro. *Science*, 348(6236): 808–812, 2015.
26. Robert Mahen, Anand D Jeyasekharan, Nicholas P Barry, and Ashok R Venkitaraman. Continuous polo-like kinase 1 activity regulates diffusion to maintain centrosome self-organization during mitosis. *Proceedings of the National Academy of Sciences*, 108(22): 9310–9315, 2011.
27. Kazuhiro Kishi, Marcel ATM Van Vugt, Ken-ichi Okamoto, Yasunori Hayashi, and Michael B Yaffe. Functional dynamics of polo-like kinase 1 at the centrosome. *Molecular and cellular biology*, 29(11):3134–3150, 2009.
28. Paul T Conduit, Alan Wainman, Zsofia A Novak, Timothy T Weil, and Jordan W Raff. Re-examining the role of drosophila sas-4 in centrosome assembly using two-colour-3d-sim frap. *Elife*, 4:e08483, 2015.
29. Paul T Conduit, Zhe Feng, Jennifer H Richens, Janina Baumbach, Alan Wainman, Suruchi D Bakshi, Jeroen Dobbelaere, Steven Johnson, Susan M Lea, and Jordan W Raff. The centrosome-specific phosphorylation of cnn by polo/plk1 drives cnn scaffold assembly and centrosome maturation. *Developmental cell*, 28(6):659–669, 2014.
30. Midori Ohta, Zhiling Zhao, Di Wu, Shaohe Wang, Jennifer L Harrison, J Sebastián Gómez-Cavazos, Arshad Desai, and Karen F Oegema. Polo-like kinase 1 independently controls microtubule-nucleating capacity and size of the centrosome. *Journal of Cell Biology*, 220 (2), 2021.
31. Ryoji Hamanaka, Mark R Smith, Patrick M O'Connor, Sharon Maloid, Kelly Mihalic, Jerry L Spivak, Dan L Longo, and Douglas K Ferris. Polo-like kinase is a cell cycle-regulated kinase activated during mitosis. *Journal of Biological Chemistry*, 270(36):21086–21091, 1995.
32. Takeshi Uchiumi, Dan L Longo, and Douglas K Ferris. Cell cycle regulation of the human polo-like kinase (plk) promoter. *Journal of Biological Chemistry*, 272(14):9166–9174, 1997.
33. Gabriela Cabral, Triin Laos, Julien Dumont, and Alexander Dammermann. Differential requirements for centrioles in mitotic centrosome growth and maintenance. *Developmental Cell*, 50(3):355–366, 2019.
34. Daniel T Gillespie. Exact stochastic simulation of coupled chemical reactions. *The Journal of Physical Chemistry*, 81(25):2340–2361, 1977.
35. Danielle R Hamill, Aaron F Severson, J Clayton Carter, and Bruce Bowerman. Centrosome maturation and mitotic spindle assembly in c. elegans require spd-5, a protein with multiple coiled-coil domains. *Developmental cell*, 3(5):673–684, 2002.
36. Hannes Fischer, Igor Polikarpov, and Aldo F Craievich. Average protein density is a molecular-weight-dependent function. *Protein Science*, 13(10):2825–2828, 2004.
37. Oliver Wueseke, David Zwicker, Anne Schwager, Yao Liang Wong, Karen Oegema, Frank Jülicher, Anthony A Hyman, and Jeffrey B Woodruff. Polo-like kinase phosphorylation determines caenorhabditis elegans centrosome size and density by biasing spd-5 toward an assembly-competent conformation. *Biology Open*, 5(10):1431–1440, 2016.
38. Maria Ana Gomez-Ferreria, Uttama Rath, Daniel W Buster, Sumit K Chanda, Jeremy S Caldwell, Daniel R Rines, and David J Sharp. Human cep192 is required for mitotic centrosome and spindle assembly. *Current Biology*, 17(22):1960–1966, 2007.
39. Ka-Wing Fong, Yuk-Kwan Choi, Jerome B Rattner, and Robert Z Qi. Cdk5rap2 is a pericentriolar protein that functions in centrosomal attachment of the $\gamma$-tubulin ring complex. *Molecular biology of the cell*, 19(1):115–125, 2008.
40. Heidi A Lane and Erich A Nigg. Antibody microinjection reveals an essential role for human polo-like kinase 1 (plk1) in the functional maturation of mitotic centrosomes. *The Journal of cell biology*, 135(6):1701–1713, 1996.

## Methods

**Stochastic growth simulations**. We use the Gillespie algorithm (34) to simulate the stochastic growth of one or multiple structures from a common pool of subunits. At any time $t$ the Gillespie algorithm uses two random variables drawn from an uniform distribution ($r_1, r_2 \in \mathcal{U}(0,1)$), and the instantaneous propensities for all of the possible reactions to update the system in time according to the defined growth law. The propensities of the relevant reactions, i.e., the assembly and disassembly rates of the $i^{th}$ structure are given by $K_i^{\text{on}}$ and $K_i^{\text{off}}$ respectively. For our growth model these propensities are functions of subunit pool size ($N$) and structure size ($n_i$),

$$K_i^{\text{on}} = k^+ \left( \frac{N - \sum_{i=1}^{M} n_i}{V} \right) , \quad \textbf{(3)}$$

$$K_i^{\text{off}} = k^- n_i^{\beta} , \quad \textbf{(4)}$$

where we are considering growth of $M$ structures from a shared pool. The Gillespie algorithm computes the time for the next reaction at $t+\tau$ given the current state of the system (i.e., the propensities for all reactions) at time $t$ where $\tau$ is given by-

$$\tau = \frac{1}{\sum_{i=1}^{C} \mathcal{R}_i} \log \left( \frac{1}{r_1} \right) , \quad \textbf{(5)}$$

where $\mathcal{R}_i$ is the propensity of $i^{th}$ reaction and $C$ is the total number of all possible reactions. The second random variable $r_2$ is used to select the particular reaction ($j^{th}$ reaction) that will occur at $t+\tau$ time such that

$$\frac{\sum_{i=1}^{j-1} \mathcal{R}_i}{\sum_{i=1}^{C} \mathcal{R}_i} \leq r_2 < \frac{\sum_{i=1}^{j} \mathcal{R}_i}{\sum_{i=1}^{C} \mathcal{R}_i} . \quad \textbf{(6)}$$

The condition for the first reaction ($j = 1$) is $0 \leq r_2 < \frac{\mathcal{R}_1}{\sum_{i=1}^{C} \mathcal{R}_i}$. The two steps defined by Eq. 5 and Eq. 6 are used recursively to compute the growth dynamics in time.

**Subunit size estimation**. Though we use single subunit and two subunit models of growth, we have used same value for the volume occupied by the subunit $\delta v$. We estimate the value of $\delta v$ from the molecular weight of SPD-5 which is 135 kDa (35). Taking the protein mass density to be $1.4$ gcc$^{-1}$ (36) and the PCM volume fraction to be $\sim 0.1$ (26), we estimate the volume occupied by SPD-5 in PCM to be $0.1 \times 162 \times 10^{-7}\,\mu\text{m}^3 \sim 2 \times 10^{-4}\,\mu\text{m}^3$.

## Acknowledgements

We thank Jordan Raff and Zachary Wilmott for many useful discussions. SB acknowledges support from the National Institutes of Health (NIH R35 GM143042) and the David Scaife Foundation.

## Acknowledgements

SB and DSB designed and developed the theory. DSB performed numerical simulations and analyzed the data. DSB and SB wrote the paper.

**Table 1.** Parameter values

| Figure | Parameter Values |
|---|---|
| Fig. 1C | $\rho_0(=N/V_c)$=0.033 $\mu$M, $k_0^+$= 600 $\mu\text{M}^{-1}\,s^{-1}$, $k_1^+$= 0.6 $\mu\text{M}^{-1}\,s^{-1}$ |
| Fig. 2A | $\rho_0$=0.033 $\mu$M |
| Fig. 2D | $k^+$=1000 $\mu\text{M}^{-1}\,s^{-1}$, $\rho_0$=0.1 $\mu$M |
| Fig. 3C | $\rho_0$ = 1 $\mu$M, $[E]$ = 0.1 $\mu$M, $k^+ = 1\,\mu\text{M}^{-1}s^{-1}$, $k^* = 1000\,\mu\text{M}^{-1}s^{-1}$, $k_E^* = 5\,s^{-1}$, $k_1^* = 1\,\mu\text{M}^{-1}s^{-1}$ |
| Fig. 3D | $\rho_0$ = 0.05 $\mu$M, $[E]$ = 0.1 $\mu$M, $k^+ = 1\,\mu\text{M}^{-1}s^{-1}$, $k^* = 2000\,\mu\text{M}^{-1}s^{-1}$, $k_E^* = 10\,s^{-1}$, $k_1^* = 100\,\mu\text{M}^{-1}s^{-1}$ |
| Fig. 3E | $\rho_0$ = 0.02 $\mu$M, $[E]$ = 0.09 $\mu$M, $k^+ = 1\,\mu\text{M}^{-1}s^{-1}$, $k^* = 8\times10^4\,\mu\text{M}^{-1}s^{-1}$, $k_E^* = 4.25\,s^{-1}$, $k_1^* = 0.1\,\mu\text{M}^{-1}s^{-1}$ |
| Fig. 3F | $\rho_0$ = 1 $\mu$M, $k^* = 1000\,\mu\text{M}^{-1}s^{-1}$, $k_E^* = 5\,s^{-1}$, $k_1^* = 10\,\mu\text{M}^{-1}s^{-1}$ |
| Fig. 3G & H | $\rho_0$ = 0.15 $\mu$M, $[E]$ = 0.085 $\mu$M, $k^+ = 1\,\mu\text{M}^{-1}s^{-1}$, $k^* = 1000\,\mu\text{M}^{-1}s^{-1}$, $k_E^* = 1\,s^{-1}$, $k_1^* = 5\,\mu\text{M}^{-1}s^{-1}$ |
| Fig. 4A | Same as Fig. 3E |
| Fig. 4B | $\rho_0$ = 0.1 $\mu$M, $[E]$ = 0.05 $\mu$M, $k^+ = 100\,\mu\text{M}^{-1}s^{-1}$, $k^* = 2000\,\mu\text{M}^{-1}s^{-1}$, $k_E^* = 10\,s^{-1}$, $k_1^* = 100\,\mu\text{M}^{-1}s^{-1}$ |
| Fig. 4D | $\rho_0$ = 0.02 $\mu$M, $[E_{ss}^*]$ = 0.01 $\mu$M, $k_1^* = 0.1\,\mu\text{M}^{-1}s^{-1}$, $V_c = 25000\,\mu\text{m}^3$ |
| Fig. 5B & D | $\rho_0$ = 0.5 $\mu$M, $[E]$ = 0.1 $\mu$M, $k^+ = 60\,\mu\text{M}^{-1}s^{-1}$, $k^* = 2000\,\mu\text{M}^{-1}s^{-1}$, $k_E^* = 10\,s^{-1}$, $k_1^* = 100\,\mu\text{M}^{-1}s^{-1}$ |
| Fig. 5C & E | $\rho_0$=0.033 $\mu$M, $k_0^+$= 60 $\mu\text{M}^{-1}\,s^{-1}$, $k_1^+$= 0.6 $\mu\text{M}^{-1}\,s^{-1}$ |
| Fig. 6B | $[\rho_a]$ = 0.25 $\mu$M, $[\rho_b]$ = 0.35 $\mu$M, $[\rho_E]$ = 0.015 $\mu$M, other parameters are same as below |
| Fig. 6C & D | $[\rho_a]$ = 0.25 $\mu$M, $[\rho_b]$ = 0.5 $\mu$M, $[\rho_E]$ = 0.01 $\mu$M, $k_a^+ = 10\,\mu\text{M}^{-1}s^{-1}$ $k_{b0}^+ = 0.5\,\mu\text{M}^{-1}s^{-1}$, $k_{b0}^- = 0.01\,s^{-1}$, |
| | $k_{aE}^+ = 5\times10^3\,\mu\text{M}^{-1}s^{-1}$, $k_{Eb}^+ = 10^3\,\mu\text{M}^{-1}s^{-1}$ $k_{b1}^+ = 10^4\,\mu\text{M}^{-1}s^{-1}$, $k_{b1}^- = 5\times10^{-3}\,s^{-1}$, $k_a^- = 5\times10^{-3}\,s^{-1}$ |
| Fixed parameters | $\delta v = 2\times10^{-4}\,\mu\text{m}^3$, $V_0 = 5\times10^{-3}\,\mu\text{m}^3$, $k^- = 5\times10^{-3}\text{s}^{-1}$, $V_c = 5000\,\mu m^3$ |

**Table 2.** Two component growth model across organisms

| | Component $a$ | Component $b$ | Enzyme $E$ | Reference |
|---|---|---|---|---|
| Fly | DSpd-2/Spd-2 | Cnn | Polo | (7, 12, 29) |
| Worm | SPD-2 | SPD-5 | PLK-1 | (25, 37) |
| Vertebrate | Cep192 | Cdk5Rap2/Cep215 | Plk1 | (38–40) |